

C_2 -symmetric *ansa* metallocenes of titanium and zirconium with a ligand system that yields pure *rac* isomer: preparation and crystal structures of $rac\text{-}\{(\eta^5\text{-C}_5\text{H}_2\text{-2-SiMe}_3\text{-4-CMe}_3)_2\text{SiMe}_2\}\text{MCl}_2$ (M = Ti or Zr) [☆]

Stephanie T. Chacon, E. Bryan Coughlin, Lawrence M. Henling, John E. Bercaw ^{*}

Arnold and Mabel Beckman Laboratories of Chemistry, California Institute of Technology, Pasadena, CA 91125, USA

Received 24 January 1995

Abstract

The preparation and structures of *rac*-[bis(2-trimethylsilyl-4-tert-butyl- η^5 -cyclopentadienyl)dimethylsilane]dichlorotitanium and *rac*-[bis(2-trimethylsilyl-4-tert-butyl- η^5 -cyclopentadienyl)dimethylsilane]dichlorozirconium, *rac*-BpMCl₂ (Bp = $\{(\eta^5\text{-C}_5\text{H}_2\text{-2-SiMe}_3\text{-4-CMe}_3)_2\text{SiMe}_2\}$; M = Ti or Zr) are described. The structures are analogous, although as expected, longer Zr atom distances result in less steric crowding. Repulsions of ring substituents on opposing rings can be seen by the differing angles about the α trimethylsilyl substituents. The [MCl₂] and SiC₂ planes of the [SiMe₂] bridge are twisted by 11° owing to intramolecular steric repulsions.

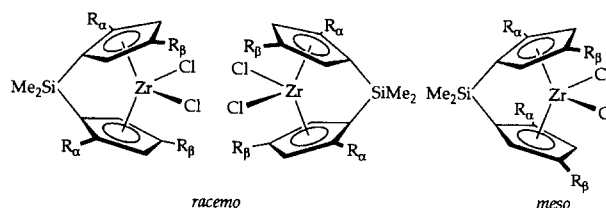
Keywords: Titanium; Zirconium; *rac-ansa* Metallocenes

1. Introduction

The relatively well-defined Ziegler–Natta propylene polymerization catalysts based on *ansa*-metallocene dichlorides of titanium, zirconium and hafnium, developed by Brintzinger and coworkers [1], in combination with methylalumoxane cocatalysts developed by Kaminsky and coworkers [2], have heralded a rebirth of interest in this important catalytic process. By tailoring the structure of the *ansa*-metallocene pre-catalyst, predictable changes in the polypropylene structure may be introduced [3]. Highly isotactic polypropylene is generally obtained using C_2 -symmetric *ansa*-metallocene dichloride catalyst precursors, e.g. with *rac*-ethylene-bis(tetrahydroindenyl)zirconocene dichloride (see Scheme 1 overleaf). Unfortunately, it is generally the case that in their preparation the C_s *meso* isomers are obtained in comparable amounts with the desired C_2 *racemo* isomer. Since the *meso* isomer produces atactic

polypropylene, separation of *racemo* and *meso* isomers must be effected in order to obtain exclusively the more desirable isospecific catalyst precursor.

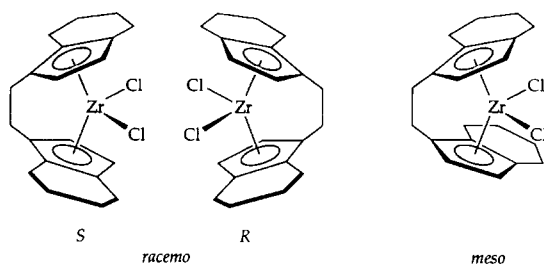
Brintzinger and co-workers have noted that, for the [SiMe₂]-bridged zirconocenes shown below, for $R_\alpha = \text{H}$ the *racemo*:*meso* ratio remains at approximately 1:1, even for relatively bulky R_β substituents such as CMe₃, SiMe₃ and CMe₂Ph. Apparently, the more open β positions have sufficient volume to accommodate even large groups in the eclipsed (or nearly eclipsed) arrangement of the *meso* isomer:



On the contrary, substitution of methyl for hydrogen at the R_α positions resulted in a considerable increase in the yield of the *racemo* isomer (*racemo*:*meso* = 2:1 for $R_\alpha = \text{CH}_3$, $R_\beta = \text{CMe}_3$, and 6:1 for $R_\alpha = \text{CH}_3$,

[☆] Dedicated by his first student (J.E.B.) to the “father” of *ansa* metallocenes, Hans-H. Brintzinger, on the occasion of his 60th birthday.

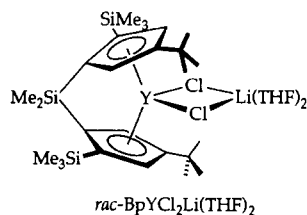
^{*} Corresponding author.



Scheme 1.

$R_{\beta} = \text{CHMe}_2$). Similar findings have been reported for a large class of $[\text{SiMe}_2]$ -linked *ansa*-zirconocenes and hafnocenes; methyl substitution at one of the α positions of each cyclopentadienyl ring favorably influences the *racemo*:*meso* ratio [4]. Reasoning that an eclipsed arrangement for R_{α} substituents larger than methyl could possibly make the *meso* isomer prohibitively crowded in the narrow portion of the metallocene wedge and thus direct the ligand attachment exclusively to the desired *racemo* isomer, we undertook the synthesis of $\{(\text{C}_5\text{H}_2-2-\text{SiMe}_3-4-\text{CMe}_3)_2\text{SiMe}_2\}\text{M}_2$ ($\text{M} = \text{Li}$ or K). We have previously reported that the *racemo* isomeric form of the ytrocene complex, $\text{BpYCl}_2\text{Li}(\text{THF})_2$, is obtained when $\text{YCl}_3(\text{THF})_3$ is treated with BpLi_2 ($\text{Bp} = \{(\text{C}_5\text{H}_2-2-\text{SiMe}_3-4-\text{CMe}_3)_2\text{SiMe}_2\}$) [5]:

$\text{YCl}_3(\text{THF})_3$ is treated with BpLi_2 ($\text{Bp} = \{(\text{C}_5\text{H}_2-2-\text{SiMe}_3-4-\text{CMe}_3)_2\text{SiMe}_2\}$).⁵

*rac*-BpYCl₂Li(THF)₂

Other strategies to favor the preferred *racemo* isomer have recently been reported. Herrmann et al. [6] have treated $\text{M}(\text{NR}_2)_4$ ($\text{R} = \text{CH}_3$; $\text{M} = \text{Zr}$ ($\text{R} = \text{CH}_3$); $\text{M} = \text{Zr}$ ($\text{R} = \text{CH}_2\text{CH}_3$); $\text{M} = \text{Hf}$) with two equivalents of the bridged cyclopentadiene-amine or bis (cyclopentadiene) ligand $\text{C}_5\text{H}_5\text{SiMe}_2\text{XH}$ ($\text{X} = \text{NC}_6\text{H}_5$ or C_5H_4) to force formation of *rac*- $\{(\eta^5-\text{C}_5\text{H}_4)\text{SiMe}_2(\eta^1-\text{X})\}_2\text{M}$. Others have employed a stereogenic linking group to discourage formation of the (pseudo-)*meso* isomer. In some cases, enantiopure C_2 -symmetric complexes were obtained [7]. Unfortunately, some stereogenic bridges employed for related ligand systems appear to be too long to permit a C_2 -symmetric conformation [8]. Further strategies have relied on 1,2-double bridges [9] of the two appropriately substituted cyclopentadienyl groups to encourage diastereoselection in the metallocene formation [10].

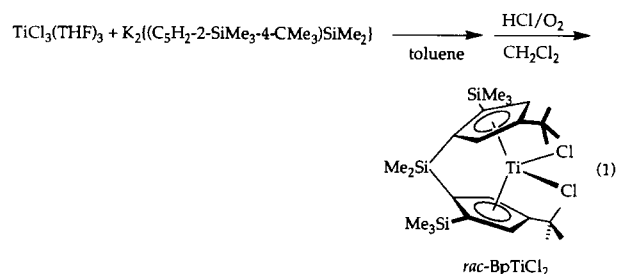
We report herein the preparation of two of the Group 4 analogs, *rac*-BpMCl₂ ($\text{M} = \text{Ti}$ or Zr), together with

the results of X-ray crystal structure determinations. Although the yield of the *ansa*-zirconocene dichloride was consistently low, exclusive formation of the desired *racemo* isomer is observed. The titanium derivative proved less problematic and, once again, exclusive formation of the *racemo* isomer is observed.

2. Results and discussion

2.1. Syntheses

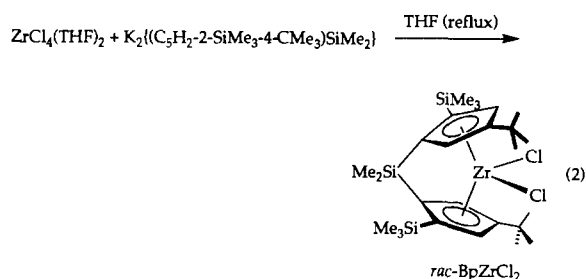
2.1.1. *rac*- $\{(\eta^5-\text{C}_5\text{H}_2-2-\text{SiMe}_3-4-\text{CMe}_3)_2\text{SiMe}_2\}\text{TiCl}_2$
rac-BpTiCl₂ was obtained in a straightforward manner by reaction of $\text{TiCl}_3(\text{THF})_3$ with K_2Bp in toluene, followed by oxidation by air in the presence of $\text{HCl}(\text{g})$:



Reaction of $\text{TiCl}_3(\text{THF})_3$ with $\text{Li}_2\text{Bp}(\text{DME})_2$ ($\text{DME} = \text{dimethoxyethane}$) followed by oxidation with PbCl_2 was also attempted, but BpTiCl_2 could not be identified among the products. In the former reaction, an aqueous HCl work-up was used initially, and the whole process was carried out in the air. Small amounts of yellow crystals formed under these conditions, presumably an oxo-bridged or hydroxo complex from reaction with atmospheric water. A yellow compound also forms upon reaction with CH_3OH . Exclusion of air and water led to better yields of BpTiCl_2 . Although ^1H NMR spectra of the crude reaction mixture after work-up indicates a much better reaction yield than the isolated yield of 44%, a further increase in isolated yield appears to be prevented by the propensity of the product to form an oil and by its high solubility in hydrocarbon solvents.

This compound was isolated as a dark-green solid. Other $\text{Ti}(\text{IV})$ *ansa*-metallocene dichloride compounds are red, purple-red or purple-brown in color. The solution appears green under laboratory fluorescent lights, but transmitted incandescent light of a flashlight is red. The UV-visible spectrum for *rac*-BpTiCl₂ is similar to those of Cp_2TiCl_2 ($\text{Cp} = (\eta^5-\text{C}_5\text{H}_5)$) and $\text{Cp}_2^*\text{TiCl}_2$ ($\text{Cp}^* = (\eta^5-\text{C}_5\text{Me}_5)$), but *rac*-BpTiCl₂ absorbs slightly more strongly in the red region and slightly less strongly in the green region, resulting in the green color of the solution of *rac*-BpTiCl₂.

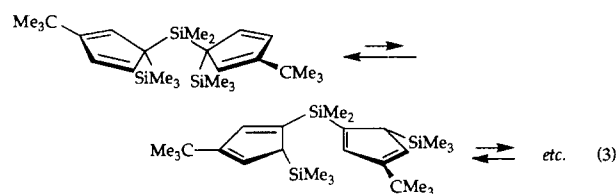
2.1.2. *rac*- $\{(\eta^5\text{-C}_5\text{H}_2\text{-2-SiMe}_3\text{-4-CMe}_3)_2\text{SiMe}_2\}\text{ZrCl}_2$
rac-BpZrCl₂ was obtained by prolonged refluxing of
 ZrCl₄(THF)₂ with K₂Bp in THF [11]:



The best yields (15% or more) were disappointing, even considering the low yields that are commonly encountered with Group 4 *ansa*-metallocene dichlorides. A variety of different procedures were tried. Reaction of K₂Bp with freshly sublimed ZrCl₄ was carried out in tetrahydrofuran (THF), toluene, methylene chloride, pentane, xylene and methylcyclohexane solutions, both at room temperature and at reflux temperatures, and even lower yields were obtained in each instance. Reaction of ZrCl₄ with Li₂Bp(DME)₂ was also attempted, but again without success. The reaction of K₂Bp with ZrCl₄(THF)₂ was carried out in benzene, toluene and THF solutions. High dilution methods were attempted; dilute solutions of each reactant were added to a large volume of solvent over many days. A mixed-solids additions technique was also used; a mixture of the solids was slowly added to a large volume of solvent at room temperature or higher temperatures. The final procedure reported gave yields many times higher than the next best method. Long reflux times are necessary. A 7 day reflux reaction led to 4% yield, a 12 day reflux reaction led to 14% yield, while the reported 25 day reflux reaction led to 15% yield. The 12 day reflux appears to be the optimal compromise. The work-up described in the experimental section was satisfactory and reproducible. Column chromatography was attempted using Florisil, alumina, silica and silanized silica (Bodman), but either no improvement in purity was found, or decomposition occurred, or both. With the silanized silica, some improvement in product purity was noted by ¹H NMR, but it was accompanied by decomposition, or overall product loss and did not yield any crystalline material. *rac*-BpZrCl₂ was found to sublime but only if almost pure, so that sublimation is not useful as a purification procedure.

During the preparation of the manuscript, we received a preprint from Jordan and coworkers [12] describing an alternate synthesis for *rac*-ethylene-1,2-bis(1-indenyl)zirconocene dichloride by reaction of Zr(NMe₂)₄ with 1,2-bis(3-indenyl)ethane, followed by reaction with Me₂NH–HCl. Unfortunately, this method

did not prove satisfactory for BpZrCl₂. A reaction between Zr(NMe₂)₄ and BpH₂ did take place, and a color change was observed; however, the reaction was incomplete and little, if any, product that had characteristic ¹H NMR signals for a [BpZr] derivative was observed. The lack of product formation probably arose from the difficulty of the deprotonation of BpH₂. Although BpH₂ appears to be present as a mixture of rapidly equilibrating double-bond isomers, the predominant isomer of each cyclopentadiene has two silicon atoms on the same (sp³-hybridized) carbon atom, and hence does not possess an acidic hydrogen:



Deprotonation of poly(silylated) cyclopentadienes has presented a general problem for us [13].

2.2. Crystal structures

Single crystals were selected from the final reaction products obtained according to Eqs. (1) and (2). The two compounds are isostructural. ORTEP drawings with 50% probability thermal ellipsoids showing the atom-numbering schemes are shown in Figs. 1 and 2 for *rac*-BpTiCl₂ and *rac*-BpZrCl₂ respectively, for one of the two enantiomers of the centrosymmetric crystals.

For both complexes the substituents on the cyclopentadienyl rings are bent upwards out of the plane of the cyclopentadienyl ring and away from the Ti or Zr. For

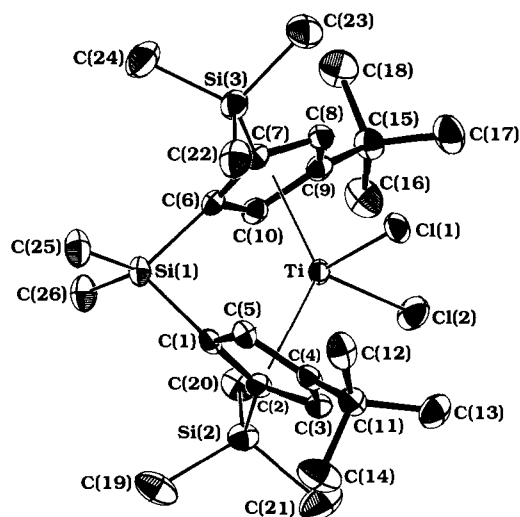


Fig. 1. ORTEP drawing of one enantiomer of *rac*-BpTiCl₂ with 50% probability ellipsoids.

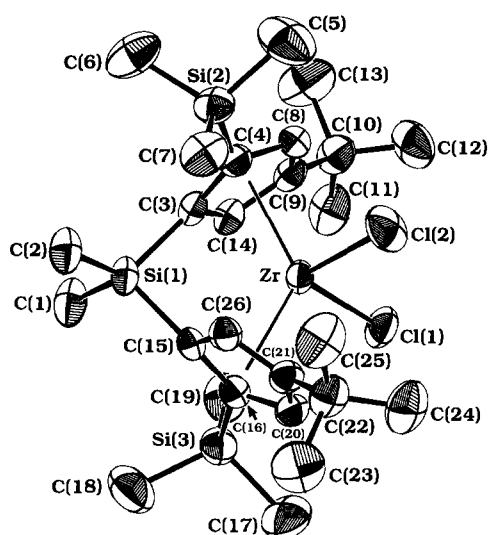


Fig. 2. ORTEP drawing of one enantiomer of *rac*-BpZrCl₂ with 50% probability ellipsoids.

the tert-butyl substituents the angles range from 10° to 11°, and for the Si(CH₃)₃ substituents the angles range from 14° to 16°. The bridging [SiMe₂] similarly is out of the cyclopentadienyl planes on the opposite side by 17° to 18° for both compounds (ring centroid–ring carbon–Si angle, 162–163°). The bridging angle about this silicon atom is also distorted; the ring carbon–Si–ring carbon atom angle is 90.8(1)° for the titanium complex and 94.0(1)° for zirconium. Other views of the two complexes looking into the metallocene wedge are shown in Fig. 3 for *rac*-BpTiCl₂ and Fig. 4 for *rac*-BpZrCl₂. These views reveal a twist of the Cl–M–Cl plane relative to the C–Si–C plane of the bridging [SiMe₂]. This twist is 11° for both complexes. We believe this twist to arise in part from steric interactions between the Cl and the tert-butyl substituents of the cyclopentadienyl rings and in part from steric interactions of the α[SiMe₂] groups with a bridging [SiMe₂] methyl and a tert-butyl substituent and α[CH] on the opposite ring. Further evidence for the high degree of steric crowding of this molecule can be seen in the angles around the α trimethylsilyl groups. For both complexes the trimethylsilyl groups show normal tetrahedral angles for the methyl groups pointing away from the wedge, but a larger angle of 117–118° for the cyclopentadienyl ring–Si–C angle for the methyl group that is directed into the wedge of the metallocene. This methyl group exhibits close non-bonded interactions with a methyl group of the [SiMe₂] linker, a chloride and an α[CH] of the opposite ring. The same magnitude of interaction is observed for *rac*-BpYCl₂Li(THF)₂ [5b].

The ring centroid–M–ring centroid angle is 130.5° for *rac*-BpTiCl₂ and 126.7° for *rac*-BpZrCl₂. Since for each compound the metal–ring carbon distances are not identical, the ring centroid–M–ring centroid angle is not equivalent to the angle between cyclopentadienyl

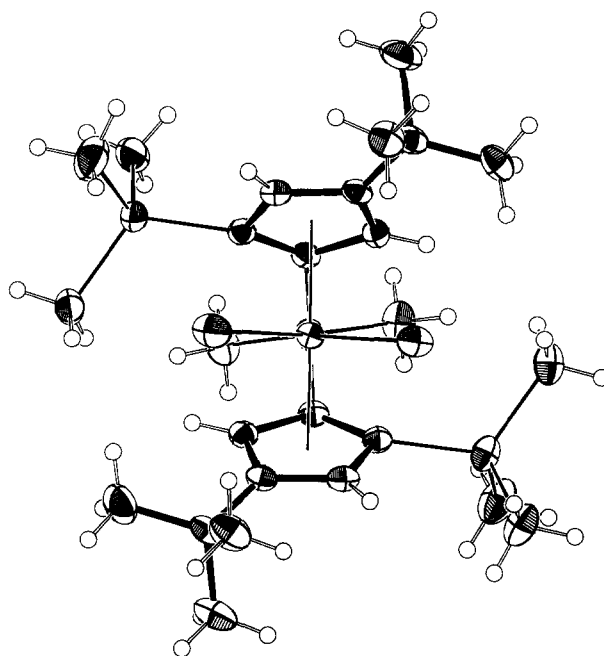


Fig. 3. ORTEP drawing of one enantiomer of *rac*-BpTiCl₂ with 50% probability ellipsoids, as viewed into the equatorial plane. Hydrogen atoms are shown to arbitrary scale.

plane normals (120.9° for *rac*-BpTiCl₂ and 117.4° for *rac*-BpZrCl₂).

3. Experimental section

TiCl₃(THF)₃, ZrCl₄(THF)₂ and HfCl₄(THF)₂ were obtained by reaction of TiCl₃, ZrCl₄ and HfCl₄, respec-

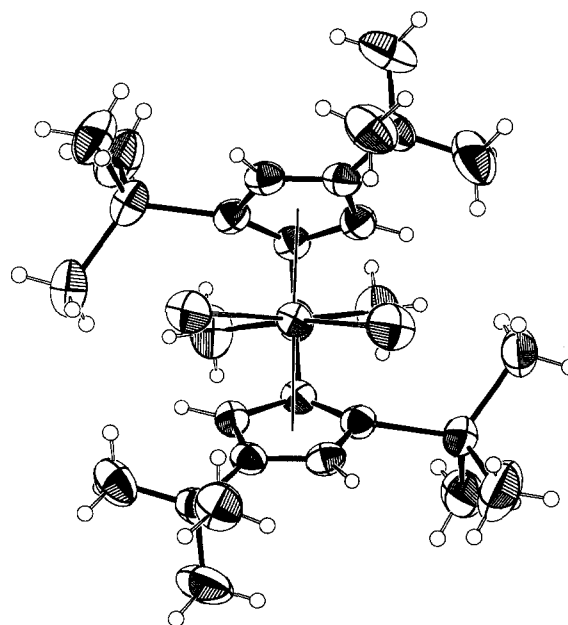


Fig. 4. ORTEP drawing of one enantiomer of *rac*-BpZrCl₂ with 50% probability ellipsoids, as viewed into the equatorial plane. Hydrogen atoms are shown to arbitrary scale.

tively with THF [14]. NMR spectra were carried out at room temperature (about 23°C) on a Bruker AM-500 spectrometer at 500 MHz for proton and 125.8 MHz for carbon. The peaks are given in chemical shift δ relative to the protio impurity in the solvent or relative to solvent nuclei for proton and carbon spectra respectively. IR spectra were taken with a Perkin–Elmer 1600 series FTIR instrument from 4400 to 450 cm^{-1} , with a resolution of 4 cm^{-1} , as KBr discs and are reported in reciprocal wavenumbers. UV–visible spectra were recorded on a Hewlett–Packard 8452A diode array spectrophotometer. Elemental analyses were carried out by Mr. Fenton Harvey on a Perkin–Elmer model 240A analyzer.

3.1. $K_2\{(C_5H_2-2-SiMe_3-4-CMe_3)_2SiMe_2\}$, K_2Bp

Dimethyl-bis(tert-butylcyclopentadienyl)silane ($[4-CMe_3C_5H_3]_2SiMe_2$) a viscous yellow liquid made by a method similar to the published procedure [1b] (10.1 g, 33.8 mmol) was placed in a 250 ml round-bottom flask equipped with a Teflon-coated stir bar and attached to a large swivel frit assembly. Petroleum ether (150 ml) was added by vacuum transfer at -78°C from titaniumocene. The solution was warmed to 0°C and 1.6 M

$n\text{-BuLi}$ in hexanes (46 ml, 74 mmol) was added by syringe. The solution was warmed to room temperature and stirred overnight. The cloudy white mixture was filtered and the white solid obtained was washed and dried in vacuo to give a 75% yield (7.88 g, 25.2 mmol) of $Li_2[4-CMe_3C_5H_3]_2SiMe_2$. ^1H NMR (THF- d_8): δ 5.85 (m, 2H, C_5H_3); 5.73 (m, 1H, C_5H_3); 1.21 (s, 9H, $C(CH_3)_3$); 0.28 (s, 3H, $Si(CH_3)_2$) ppm.

$Li_2[4-CMe_3C_5H_3]_2SiMe_2$ (7.4240 g, 0.02376 mol) was placed in a 500 ml round-bottom flask equipped with a Teflon-coated stir bar and attached to a large swivel frit equipped with another 500 ml round-bottom flask with a Teflon-coated stir bar, and a gas inlet adapter. THF (250 ml) was added by vacuum transfer at -78°C from sodium diphenyl ketyl and trimethylsilyl chloride (9 ml, 0.7 mol) was added by vacuum transfer at -78°C from calcium hydride using a graduated tube to measure the volume at room temperature. The flask was warmed to room temperature and the contents stirred overnight. The volatiles were removed in vacuo. Petroleum ether (100 ml) was added and the LiCl was removed by filtration and washed and the product was dried in vacuo to give 82% yield of $\{C_5H_3(SiMe_3)(CMe_3)\}_2SiMe_2$ (8.6414 g, 0.01942 mol), a viscous yellow oil. Owing to the large number of regioisomers

Table 1
Crystal data

Formula	$C_{26}H_{46}Cl_2Si_3Ti$	$C_{26}H_{46}Cl_2Si_3Zr$
Formula weight (g mol^{-1})	561.69	605.03
Crystal color	Green	Yellow
Crystal shape	Irregular cube	Prism
Crystal size (mm)	$0.40 \times 0.50 \times 0.60$	$0.30 \times 0.33 \times 0.37$
Crystal system	Monoclinic	Monoclinic
Space group	$P2_1/n$ (No. 14)	$P2_1/n$ (No. 14)
a (\AA)	15.413(4)	15.513(3)
b (\AA)	12.830(3)	13.075(2)
c (\AA)	17.122(4)	17.243(3)
β ($^\circ$)	122.24(2)	111.18(2)
Volume (\AA^3)	3134(1)	3261(1)
Z (molecule cell^{-1})	4	4
ρ_{calc} (g cm^{-3})	1.19	1.23
μ (cm^{-1})	5.67	6.17
Diffractometer	Enraf–Nonius CAD4	Enraf–Nonius CAD4
Temperature (K)	170	295
λ (Mo $K\alpha$) (\AA)	0.71073	0.71073
2θ range ($^\circ$)	2–50	2–46
Scan type	ω – 2θ	ω – 2θ
Number of independent reflections	5515	4524
Number of reflections measured	10866	9732
Goodness of fit for merging	1.51	1.02
Range of transmission factor	–	0.97–1.03
R for reflections with $F_0^2 > 0$	0.035 (5263)	0.036 (4210)
R for reflections with $F_0^2 > 3\sigma(F_0^2)$	0.029 (4528)	0.029 (3683)
Goodness of fit	2.02	1.88
Number of parameters	473	290
$(\Delta/\sigma)_{\text{max}}$ in final least-squares cycle	0.01	0.01
$\Delta\rho_{\text{max}}; \Delta\rho_{\text{min}}$ (electrons \AA^{-3})	+0.66; –0.26	+0.33; –0.29

resulting from silyl migrations about the cyclopentadienyl rings, ^1H NMR spectra were complicated. Upon standing for several weeks, the yellow liquid changes to a low melting solid.

$(\text{C}_5\text{H}_3(\text{SiMe}_3)(\text{CMe}_3))_2\text{SiMe}_2$ (13.90 g, 30.4 mmol) was dissolved in THF (300 ml) in a nitrogen atmosphere glove-box. KOCMe_3 (6.82 g, 60.8 mmol) was added, and the reaction stirred at room temperature for 22 h. The volatiles were removed in vacuo. The resulting solid was powdered, and the powder was heated to 60°C under dynamic vacuum overnight to remove the last traces of Me_3COH .

$\text{K}_2\{(\text{C}_5\text{H}_2-2-\text{SiMe}_3-4-\text{CMe}_3)_2\text{SiMe}_2\}$ was thus obtained with a 93% yield (14.67 g, 28.15 mmol).

^1H NMR (benzene- d_6): δ 6.36 (d, 1H, $^4J_{\text{H-H}} = 2$ Hz, C_5H_2); 6.09 (d, 1H, $^4J_{\text{H-H}} = 2$ Hz, C_5H_2); 1.29 (s, 1H, $\text{C}(\text{CH}_3)_3$); 1.09 (s, 3H, $\text{Si}(\text{CH}_3)_2$); 0.54 (s, 9H, $\text{Si}(\text{CH}_3)_3$). IR (cm^{-1}): δ 3090(m), 3060(w), 2975(vs), 2940(sh), 2905(vs), 2880(vs), 1730(w), 1715(w), 1675(w), 1580(m), 1495(s), 1480(vs), 1418(m), 1402(sh), 1380(vs), 1348(w), 1338(w), 1280(vs), 1220(m), 1155(vs), 1130(m), 1110(m), 1055(vs), 1015(m), 992(vs), 920(s), 910(s), 890(vs), 820(vs, broad), 784(vs), 755(s), 745(s), 720(m), 690(s), 670(vs), 620(m), 608(w), 510(m), 500(w), 485(w) cm^{-1} . Elemental Anal. $\text{WO}_3\text{-V}_2\text{O}_5$ added to aid combustion. Found: C, 59.45, 60.80; H, 8.93, 8.92; $\text{C}_{26}\text{H}_{46}\text{K}_2\text{Si}_3$ Calc.: C, 59.93; H, 8.90%.

3.2. *rac-BpTiCl_2*

$\text{TiCl}_3(\text{THF})_3$ (1.4441 g, 3.897 mmol) and $\text{K}_2\{(\text{C}_5\text{H}_2-2-\text{SiMe}_3-4-\text{CMe}_3)_2\text{SiMe}_2\}$ (2.0308 g, 3.897 mmol) were placed in a 250 ml Kjeldahl flask equipped with a Teflon-coated stir bar and a reflux condenser with a gas inlet tube on top. Toluene (100 ml) was vacuum transferred from titanocene at -78°C . The flask was allowed to warm slowly to room temperature overnight. The initial color of the solution was light blue. At -45°C the color changed to green, and it was brown by -25°C . The solution was heated to reflux for 2.5 h, and the solvent was removed in vacuo. Methylene chloride (50 ml) was added by vacuum transfer from calcium hydride at -78°C . Hydrogen chloride gas was bubbled through the solution by cannula, and the flask was opened to the air to allow oxidation to take place. During this time the color of the solution changed from red-brown to emerald green. After stirring for 10 min the solvent was removed in vacuo. The flask was attached to a swivel frit assembly and evacuated. Pentane (75 ml) was added by vacuum transfer from sodium diphenyl ketyl at -78°C , and the mixture was filtered and washed to remove the KCl precipitate. The volume of the solution was reduced to 25 ml and allowed to stand overnight. The solution was cooled to -78°C for 2 h and filtered to isolate 448 mg of green crystals. The

volume of the solution was reduced further and the flask was placed in a freezer at -55°C for 2 days. More green crystals (236 mg) were isolated by pipetting off the supernatant. Further crystallization of the mother liquor from benzene-pentane mixtures lead to five more batches of crystals totaling 277 mg to give a final yield of 44% (961 mg, 1.71 mmol).

^1H NMR (benzene- d_6): δ 7.46 (d, $^4J_{\text{H-H}} = 2$ Hz, 2H, C_5H_2); 5.98 (d, $^4J_{\text{H-H}} = 2$ Hz, 2H, C_5H_2); 1.43 (s, 18H, $\text{C}(\text{CH}_3)_3$); 0.60 (s, 6H, $\text{Si}(\text{CH}_3)_2$); 0.33 (s, 18H, $\text{Si}(\text{CH}_3)_3$) ppm. ^{13}C NMR (benzene- d_6): δ 162.7 (s, C_5H_2 -*ipso*); 142.4 (dd, $^1J_{\text{C-H}} = 173$ Hz, $^3J_{\text{C-H}} = 8$ Hz); 136.4 (s, C_5H_2); 119.5 (dd, $^1J_{\text{C-H}} = 168$ Hz, $^3J_{\text{C-H}} = 9$ Hz); 111.2 (s, C_5H_2); 35.1 (s, $\text{C}(\text{CH}_3)_3$); 30.1 (q, $^1J_{\text{C-H}} = 127$ Hz, $\text{C}(\text{CH}_3)_3$); 2.2 (q, $^1J_{\text{C-H}} = 120$ Hz, $\text{Si}(\text{CH}_3)_3$); -1.3 (q, $^1J_{\text{C-H}} = 123$ Hz, $\text{Si}(\text{CH}_3)_2$) ppm. IR: δ 2960(s), 2900(m), 2860(sh), 1505(m), 1480(m), 1420(w), 1390(w), 1365(m), 1360(m), 1270(s), 1190(m), 1140(w), 1100(m), 990(m), 970(w), 870(sh), 860(vs), 820(m), 805(m), 780(m), 700(m), 660(m), 510(m) cm^{-1} . UV-visible: λ_{max} (ϵ) 256(12000), 282(15000), 612 nm ($270 \text{ M}^{-1} \text{cm}^{-1}$).

Table 2
Final heavy-atom parameters for BpTiCl_2

Atom	x ($\times 10^{-4}$)	y ($\times 10^{-4}$)	z ($\times 10^{-4}$)	U_{eq}^a ($\times 10^{-4} \text{ \AA}^2$)
Ti	2337(0.2)	2518(0.2)	4780(0.2)	196(1)
Cl(1)	2008(0.3)	3349(0.4)	3481(0.3)	304(1)
Cl(2)	776(0.3)	2202(0.4)	4583(0.4)	394(1)
Si(1)	4348(0.3)	2024(0.4)	6302(0.3)	236(1)
Si(2)	2168(0.4)	2501(0.4)	6999(0.3)	285(1)
Si(3)	4310(0.4)	2082(0.5)	3935(0.3)	296(1)
C(1)	3453(1)	3083(1)	6094(1)	215(4)
C(2)	2553(1)	3068(1)	6167(1)	227(4)
C(3)	2024(1)	3892(1)	5642(1)	243(4)
C(4)	2543(1)	4413(1)	5250(1)	236(4)
C(5)	3414(1)	3878(1)	5499(1)	227(4)
C(6)	3617(1)	1354(1)	5295(1)	229(4)
C(7)	3491(1)	1596(1)	4437(1)	229(4)
C(8)	2626(1)	1115(2)	3918(1)	250(4)
C(9)	2220(1)	585(1)	4406(1)	243(4)
C(10)	2808(1)	782(1)	5257(1)	241(4)
C(11)	2292(1)	5463(2)	4813(1)	284(5)
C(12)	2876(2)	5733(2)	4296(1)	346(6)
C(13)	1242(2)	5536(2)	4266(2)	382(6)
C(14)	2525(2)	6255(2)	5542(2)	490(8)
C(15)	1427(1)	-213(2)	4068(1)	297(5)
C(16)	1017(2)	-492(2)	4725(2)	447(6)
C(17)	658(2)	141(2)	3246(2)	434(6)
C(18)	1897(2)	-1191(2)	3886(2)	473(7)
C(19)	3069(2)	2940(2)	8017(2)	437(7)
C(20)	1975(2)	1069(2)	6984(2)	358(5)
C(21)	1018(2)	3106(3)	6853(2)	532(7)
C(22)	4536(2)	3507(2)	3975(2)	384(5)
C(23)	3774(2)	1705(2)	2807(2)	447(6)
C(24)	5441(2)	1364(2)	4422(2)	483(6)
C(25)	5487(1)	2567(2)	6362(1)	358(6)
C(26)	4536(2)	1175(2)	7226(1)	336(5)

^a $U_{\text{eq}} = \frac{1}{3} \sum_i \sum_j [U_{ij}(a_i^* a_j^* \chi(a_i \cdot a_j))]$.

Elemental Anal. Found: C, 55.22; H, 7.92; $\text{WO}_3\text{-V}_2\text{O}_5$ added to aid combustion $\text{C}_{26}\text{H}_{46}\text{Cl}_2\text{Si}_3\text{Ti}$ Calc.: C, 55.60; H, 8.25.

3.3. *rac*-BpZrCl₂

ZrCl₄(THF)₂ (1.4432 g; 3.826 mmol) and K₂{(C₅H₂-2-SiMe₃-4-CMe₃)₂SiMe₂} (1.9935 g; 3.826 mmol) were placed in a 200 ml Kjeldahl flask equipped with a Teflon-coated stir bar and a reflux condenser with a gas inlet tube on top. THF (125 ml) was vacuum transferred from sodium diphenyl ketyl at -78°C. The flask was allowed to warm to reflux; during 25 days the color changed from tan to a gradually deepening yellow. The solvent was removed in vacuo to yield a dark-yellow solid. Methylene chloride (30 ml) and 6 M HCl (4 ml) were added to yield a yellow-brown solution and a white precipitate. At this time the flask was opened to the air and more 6 M HCl (26 ml) was added to dissolve the precipitate and the product was extracted. The green-brown organic phase was extracted with 2 × 20 ml 6 M HCl, and the pale-yellow aqueous phase with 3 × 10 ml of methylene chloride. The combined

organic phase was dried over anhydrous sodium sulfate, filtered and the solvent removed in vacuo to yield an orange brown oil. Crystals were obtained from 15% HCl in methanol: benzene 5:1 v:v by slow evaporation. Washing with pentane and 15% HCl in methanol gave a total yield of 15% (327 mg, 0.541 mmol) in three batches. ¹H NMR (benzene-*d*₆): δ 7.22 (d, ⁴J_{H-H} = 2 Hz, 2H, C₅H₂); 6.16 (d, ⁴J_{H-H} = 2 Hz, 2H, C₅H₂); 1.39 (s, 18H, C(CH₃)₃); 0.64 (s, 6H, Si(CH₃)₂); 0.36 (s, 18H, Si(CH₃)₃) ppm. ¹H NMR (toluene-*d*₈): δ 7.10 (d, ⁴J_{H-H} = 2 Hz, 2H, C₅H₂); 6.13 (d, ⁴J_{H-H} = 2 Hz, 2H, C₅H₂); 1.37 (s, 18H, C(CH₃)₃); 0.68 (s, 6H, Si(CH₃)₂); 0.36 (s, 18H, Si(CH₃)₃) ppm. ¹H NMR (THF-*d*₈): δ 6.97 (d, ⁴J_{H-H} = 2 Hz, 2H, C₅H₂); 6.08 (d, ⁴J_{H-H} = 2 Hz, 2H, C₅H₂); 1.31 (s, 18H, C(CH₃)₃); 0.89 (s, 6H, Si(CH₃)₂); 0.32 (s, 18H, Si(CH₃)₃) ppm. ¹³C[¹H] NMR (benzene-*d*₆): δ 156.9 (C₅H₂-*ipso*); 135.2 (C₅H₂); 131.2 (C₅H₂); 117.1 (C₅H₂); 113.6 (C₅H₂); 34.2 (C(CH₃)₃); 30.4 (C(CH₃)₃); 2.2 (Si(CH₃)₃); -0.8 (Si(CH₃)₂) ppm. IR: 2980(s), 2905(w), 2885(w), 1495(w), 1458(w), 1408(w), 1392(w), 1358(m), 1352(w), 1250(vs), 1200(sh), 1178(s), 1128(w), 1090(m), 976(s), 949(w), 870(sh), 847(vs), 828(vs),

Table 3
Selected distances (Å) and angles (°) for BpTiCl₂

Distances					
Ti-Cl(1)	2.343(1)	Si(3)-C(7)	1.883(2)	C(7)-C(8)	1.432(3)
Ti-Cl(2)	2.335(1)	Si(3)-C(22)	1.857(3)	C(8)-C(9)	1.396(3)
Ti-Cp(1)	2.109	Si(3)-C(23)	1.854(3)	C(9)-C(10)	1.418(3)
Ti-Cp(2)	2.112	Si(3)-C(24)	1.865(3)	C(9)-C(15)	1.530(3)
Si(1)-C(1)	1.873(2)	C(1)-C(2)	1.439(3)	C(11)-C(12)	1.523(3)
Si(1)-C(6)	1.873(2)	C(1)-C(5)	1.426(3)	C(11)-C(13)	1.536(3)
Si(1)-C(25)	1.855(2)	C(2)-C(3)	1.427(3)	C(11)-C(14)	1.542(3)
Si(1)-C(26)	1.851(2)	C(3)-C(4)	1.395(3)	C(15)-C(16)	1.529(3)
Si(2)-C(2)	1.885(2)	C(4)-C(5)	1.421(3)	C(15)-C(17)	1.526(3)
Si(2)-C(19)	1.858(3)	C(4)-C(11)	1.518(3)	C(15)-C(18)	1.538(4)
Si(2)-C(20)	1.860(3)	C(6)-C(7)	1.441(3)		
Si(2)-C(21)	1.862(3)	C(6)-C(10)	1.427(3)		
Angles					
Cl(1)-Ti-Cl(2)	95.8(0.2)	C(24)-Si(3)-C(7)	107.8(1)	C(8)-C(7)-C(6)	106.0(2)
Cp(1)-Ti-Cp(2)	130.5	C(23)-Si(3)-C(22)	107.4(1)	C(9)-C(8)-C(7)	111.2(2)
Cp(1)-Ti-Cl(1)	107.6	C(24)-Si(3)-C(22)	109.9(1)	C(10)-C(9)-C(8)	105.8(2)
Cp(1)-Ti-Cl(2)	105.1	C(24)-Si(3)-C(23)	108.0(1)	C(15)-C(9)-C(8)	125.0(2)
Cp(2)-Ti-Cl(1)	104.4	C(2)-C(1)-Si(1)	129.7(1)	C(15)-C(9)-C(10)	128.1(2)
Cp(2)-Ti-Cl(2)	108.1	C(5)-C(1)-Si(1)	118.9(1)	C(9)-C(10)-C(6)	110.3(2)
C(6)-Si(1)-C(1)	90.8(1)	C(5)-C(1)-C(2)	106.9(2)	C(12)-C(11)-C(4)	113.1(2)
C(25)-Si(1)-C(1)	110.6(1)	C(1)-C(2)-Si(2)	131.4(1)	C(13)-C(11)-C(4)	111.6(2)
C(26)-Si(1)-C(1)	117.1(1)	C(3)-C(2)-Si(2)	119.6(1)	C(14)-C(11)-C(4)	104.4(2)
C(25)-Si(1)-C(6)	116.7(1)	C(3)-C(2)-C(1)	105.9(2)	C(13)-C(11)-C(12)	110.5(2)
C(26)-Si(1)-C(6)	111.2(1)	C(4)-C(3)-C(2)	111.3(2)	C(14)-C(11)-C(12)	108.2(2)
C(26)-Si(1)-C(25)	109.6(1)	C(5)-C(4)-C(3)	105.8(2)	C(14)-C(11)-C(13)	108.8(2)
C(19)-Si(2)-C(2)	104.7(1)	C(11)-C(4)-C(3)	125.2(2)	C(16)-C(15)-C(9)	111.8(2)
C(20)-Si(2)-C(2)	117.7(1)	C(11)-C(4)-C(5)	127.8(2)	C(17)-C(15)-C(9)	112.4(2)
C(21)-Si(2)-C(2)	107.1(1)	C(4)-C(5)-C(1)	109.9(2)	C(18)-C(15)-C(9)	104.6(2)
C(20)-Si(2)-C(19)	111.8(1)	C(7)-C(6)-Si(1)	130.0(1)	C(17)-C(15)-C(16)	110.8(2)
C(21)-Si(2)-C(19)	109.6(1)	C(10)-C(6)-Si(1)	119.2(1)	C(18)-C(15)-C(16)	108.4(2)
C(21)-Si(2)-C(20)	105.7(1)	C(10)-C(6)-C(7)	106.6(2)	C(18)-C(15)-C(17)	108.6(2)
C(22)-Si(3)-C(7)	117.2(1)	C(6)-C(7)-Si(3)	132.9(1)		
C(23)-Si(3)-C(7)	106.1(1)	C(8)-C(7)-Si(3)	119.2(1)		

798(s), 782(s), 753(s), 680(s), 630(m), 500(s) cm^{-1} . Elemental Anal. Found: C, 51.46; H, 7.50; $\text{WO}_3\text{-V}_2\text{O}_5$ added to aid combustion. $\text{C}_{26}\text{H}_{46}\text{Cl}_2\text{Si}_3\text{Zr}$ Calc.: C, 51.61; H, 7.66%.

3.4. Structure determination for *rac*-BpTiCl₂

A fragment cut from a single crystal was epoxied to a glass fiber and centered on the diffractometer under a stream of cold nitrogen gas. Crystallographic data are presented in Tables 1, 2 and 3. Unit-cell parameters and an orientation matrix were obtained by a least-squares calculation from setting angles of 25 reflections with $12^\circ < \theta < 13.5^\circ$. Two equivalent data sets were collected. No correction was made for decay or absorption. Lorentz and polarization factors were applied, and the two data sets were then merged. Systematic absences in the diffractometer data showed the space group to be $P2_1/n$. The Ti atom coordinates were obtained from a Patterson map; the remaining non-hydrogen atoms were found in subsequent structure factor–Fourier calculations. The hydrogen atoms were located in difference Fourier maps and refined isotropically in the full-matrix least-squares refinement.

3.5. Structure determination for *rac*-BpZrCl₂

A single crystal was sealed in a capillary under nitrogen and centered on the diffractometer. Crystallographic data are presented in Tables 1, 4 and 5. Unit-cell parameters and an orientation matrix were obtained by a least-squares calculation from setting angles of 25 reflections with $12^\circ < \theta < 14^\circ$. Two equivalent data sets were collected. An empirical ψ scan method was used to correct for absorption; there was no noticeable decay. Lorentz and polarization factors were applied, and the two data sets were then merged. Systematic absences in the diffractometer data showed the space group to be $P2_1/n$. The Zr atom coordinates were obtained from a Patterson map; the remaining non-hydrogen atoms were found in subsequent structure factor–Fourier calculations. The hydrogen atoms were positioned by calculation (C–H, 0.95 Å) with $B = 1.1$ times the equivalent B of the bonded atom and repositioned during the full matrix least-squares refinement. A secondary extinction parameter ($0.49(2) \times 10^{-6}$) was included [15].

Calculations for both structures were done with programs of the CRYM Crystallographic Computing System [16] and ORTEP [17]. Scattering factors and corrections for anomalous scattering were taken from a standard reference [18]. $R = \sum |F_o - |F_c|| / \sum F_o$, for only $F_o^2 > 0$, and goodness of fit $[\sum w(F_o^2 - F_c^2)^2 / (n - p)]^{1/2}$, where n is the number of data and p is the number of parameters refined. The function minimized in least-squares was $\sum w(F_o^2 - F_c^2)^2$, where $w = 1/\sigma^2(F_o^2)$. Variances of the individual reflections were assigned based on counting statistics plus an additional term

Table 4
Final heavy-atom parameters for BpZrCl₂

Atom	x ($\times 10^{-4}$)	y ($\times 10^{-4}$)	z ($\times 10^{-4}$)	U_{eq}^a ($\times 10^{-4} \text{ \AA}^2$)
Zr	7268(0.2)	2453(0.2)	9726(0.2)	364(1)
Cl(1)	6980(0.6)	1624(0.6)	8392(0.4)	580(2)
Cl(2)	5672(0.6)	2768(0.7)	9559(0.6)	728(3)
Si(1)	9274(0.6)	2936(0.7)	11251(0.5)	436(2)
C(1)	10401(2)	2406(3)	11305(2)	658(10)
C(2)	9452(2)	3767(3)	12170(2)	614(9)
C(3)	8406(2)	1883(2)	11073(2)	385(7)
C(4)	7524(2)	1869(2)	11168(2)	415(7)
Si(2)	7132(0.7)	2428(0.7)	11995(0.5)	539(2)
C(5)	6000(3)	1844(4)	11868(3)	1082(14)
C(6)	7993(3)	1995(3)	12998(2)	849(12)
C(7)	6953(3)	3834(3)	11978(2)	700(10)
C(8)	7014(2)	1044(2)	10663(2)	440(7)
C(9)	7539(2)	547(2)	10269(2)	417(7)
C(10)	7294(2)	-484(2)	9830(2)	551(9)
C(11)	7883(3)	-722(3)	9313(2)	694(10)
C(12)	6269(3)	-555(3)	9291(2)	766(11)
C(13)	7514(4)	-1275(3)	10534(2)	984(15)
C(14)	8383(2)	1084(2)	10501(2)	410(7)
C(15)	8592(2)	3631(2)	10266(2)	388(7)
C(16)	8491(2)	3424(2)	9418(2)	419(7)
Si(3)	9316(0.6)	2949(0.8)	8921(0.6)	565(2)
C(17)	8803(3)	3298(3)	7805(2)	869(12)
C(18)	10425(3)	3648(3)	9393(3)	919(12)
C(19)	9543(2)	1551(3)	8969(2)	729(10)
C(20)	7657(2)	3923(2)	8914(2)	457(8)
C(21)	7243(2)	4437(2)	9398(2)	443(8)
C(22)	6471(2)	5223(2)	9080(2)	587(9)
C(23)	6929(3)	6191(3)	8907(3)	951(14)
C(24)	5720(3)	4881(3)	8268(2)	826(12)
C(25)	6046(3)	5471(3)	9724(2)	867(12)
C(26)	7807(2)	4219(2)	10230(2)	436(7)

$$^a U_{\text{eq}} = \frac{1}{3} \sum_i \sum_j [U_{ij}(a_i^* a_j^* \chi(a_i \cdot a_j))].$$

(0.014I)². Variances of the merged reflections were determined by the standard propagation error plus another additional term (0.014I)².

4. Supplementary material available

Tables of final parameters for the structures of *rac*-BpTiCl₂ and *rac*-BpZrCl₂, assigned hydrogen parameters, anisotropic displacement parameters, complete distances and angles, and tables of observed and calculated structure factors have been deposited at the Cambridge Crystallographic Data Centre.

Acknowledgments

The work has been supported by US Department of Energy Office of Basic Energy Sciences (Grant DE-FG03-85ER113431) and by Exxon Chemical Americas. We wish to thank William P. Schaefer for solving the *rac*-BpZrCl₂ crystal structure and Richard E. Marsh for assistance in solving the *rac*-BpTiCl₂ structure. S.T.C.

Table 5
Selected distances (Å) and angles (°) for BpZrCl₂

Distances					
Zr–Cl(1)	2.435(1)	Si(3)–C(16)	1.884(3)	C(16)–C(20)	1.429(4)
Zr–Cl(2)	2.422(1)	Si(3)–C(19)	1.857(4)	C(20)–C(21)	1.396(4)
Zr–Cp(1)	2.233	Si(3)–C(17)	1.853(4)	C(21)–C(26)	1.413(4)
Zr–Cp(2)	2.233	Si(3)–C(18)	1.857(4)	C(21)–C(22)	1.522(4)
Si(1)–C(3)	1.872(3)	C(3)–C(4)	1.436(4)	C(10)–C(11)	1.522(5)
Si(1)–C(15)	1.879(3)	C(3)–C(14)	1.428(4)	C(10)–C(12)	1.527(5)
Si(1)–C(1)	1.852(3)	C(4)–C(8)	1.432(4)	C(10)–C(13)	1.536(5)
Si(1)–C(2)	1.856(3)	C(8)–C(9)	1.396(4)	C(22)–C(25)	1.518(5)
Si(2)–C(4)	1.887(3)	C(9)–C(14)	1.410(4)	C(22)–C(24)	1.529(5)
Si(2)–C(6)	1.852(4)	C(9)–C(10)	1.525(4)	C(22)–C(23)	1.532(5)
Si(2)–C(7)	1.858(4)	C(15)–C(16)	1.439(4)		
Si(2)–(5)	1.855(5)	C(15)–C(26)	1.423(4)		
Angles					
Cl(1)–Zr–Cl(2)	97.6(0.3)	C(18)–Si(3)–C(16)	108.2(2)	C(20)–C(16)–C(15)	105.9(2)
Cp(1)–Zr–Cp(2)	126.7	C(17)–Si(3)–C(19)	107.0(2)	C(21)–C(20)–C(16)	111.5(3)
Cp(1)–Zr–Cl(1)	108.9	C(18)–Si(3)–C(19)	109.5(2)	C(26)–C(21)–C(20)	105.1(3)
Cp(1)–Zr–Cl(2)	105.4	C(18)–Si(3)–C(17)	108.4(2)	C(22)–C(21)–C(20)	125.5(3)
Cp(2)–Zr–Cl(1)	104.7	C(4)–C(3)–Si(1)	130.4(2)	C(22)–C(21)–C(26)	128.3(3)
Cp(2)–Zr–Cl(2)	109.8	C(14)–C(3)–Si(1)	119.3(2)	C(21)–C(26)–C(15)	111.0(3)
C(15)–Si(1)–C(3)	94.0(1)	C(14)–C(3)–C(4)	106.4(2)	C(11)–C(10)–C(9)	112.1(3)
C(1)–Si(1)–C(3)	110.0(1)	C(3)–C(4)–Si(2)	131.4(2)	C(12)–C(10)–C(9)	111.9(3)
C(2)–Si(1)–C(3)	116.5(1)	C(8)–C(4)–Si(2)	119.6(2)	C(13)–C(10)–C(9)	105.0(3)
C(1)–Si(1)–C(15)	116.0(1)	C(8)–C(4)–C(3)	106.2(2)	C(12)–C(10)–C(11)	110.2(3)
C(2)–Si(1)–C(15)	110.5(1)	C(9)–C(8)–C(4)	110.8(3)	C(13)–C(10)–C(11)	108.4(3)
C(2)–Si(1)–C(1)	109.3(2)	C(14)–C(9)–C(8)	105.9(2)	C(13)–C(10)–C(12)	109.0(3)
C(6)–Si(2)–C(4)	105.5(2)	C(10)–C(9)–C(8)	124.6(3)	C(25)–C(22)–C(21)	111.9(3)
C(7)–Si(2)–C(4)	117.3(2)	C(10)–C(9)–C(14)	128.4(3)	C(24)–C(22)–C(21)	111.9(3)
C(5)–Si(2)–C(4)	107.5(2)	C(9)–C(14)–C(3)	110.5(2)	C(23)–C(22)–C(21)	105.5(3)
C(7)–Si(2)–C(6)	111.7(2)	C(16)–C(15)–Si(1)	130.4(2)	C(24)–C(22)–C(25)	110.1(3)
C(5)–Si(2)–C(6)	108.5(2)	C(26)–C(15)–Si(1)	119.6(2)	C(23)–C(22)–C(25)	108.7(3)
C(5)–Si(2)–C(7)	106.0(2)	C(26)–C(15)–C(16)	106.3(2)	C(23)–C(22)–C(24)	108.5(3)
C(19)–Si(3)–C(16)	117.0(2)	C(15)–C(16)–Si(3)	133.0(2)		
C(17)–Si(3)–C(16)	106.5(2)	C(20)–C(16)–Si(3)	119.2(2)		

thanks the James K. Irvine Foundation for a research fellowship.

References and notes

- (a) W. Roll, H.H. Brintzinger, B. Rieger and R. Zolk, *Angew. Chem., Int. Edn. Engl.*, **29** (1990) 279.
(b) H. Wiesenfeldt, A. Reinmuth, E. Barsties, K. Evertz, H.H. Brintzinger, *J. Organomet. Chem.* **369** (1989) 359.
- (a) H. Sinn and W. Kaminsky, *Adv. Organomet. Chem.*, **18** (1980) 99.
(b) H. Sinn, W. Kaminsky, H.J. Vollmer and R. Woldt, *Angew. Chem., Int. Edn. Engl.*, **19** (1980) 390.
- (a) H. Schutenhaus and H.H. Brintzinger, *Angew. Chem., Int. Edn. Engl.*, **18** (1979) 777.
(b) P. Burger, K. Hortmann and H.H. Brintzinger, *Makromol. Chem.*, **66** (1993) 127.
(c) J.A. Ewen, *J. Am. Chem. Soc.*, **106** (1984) 6355.
(d) F.R.W.P. Wild, L. Zsolnai, G. Huttner, and H.H. Brintzinger, *J. Organomet. Chem.*, **232** (1982) 233.
(e) W. Kaminsky, K. Külper, H.H. Brintzinger and F.R.W.P. Wild, *Angew. Chem. Int. Edn. Engl.*, **24** (1985) 507.
(f) B. Rieger, A. Reinmuth, W. Röhl and H.H. Brintzinger, *J. Mol. Catal.*, **82** (1993) 62.
(g) W. Röhl, H.H. Brintzinger, B. Rieger and R. Zolk, *Angew. Chem., Int. Edn. Engl.*, **29** (1990) 279.
(h) B. Rieger, X. Mu, D.T. Mallin, M.D. Rausch and J.C.W. Chien, *Macromolecules*, **23** (1990) 3559.
(i) J.A. Ewen, R.L. Jones, A. Razavi and J.D.F. Ferrara, *J. Am. Chem. Soc.*, **110** (1988) 6255.
(j) J.A. Ewen, M.J. Elder, R.L. Jones, L. Haspeslagh, J.L. Atwood, S.G. Bott and K. Robinson, *Makromol. Chem., Makromol. Symp.*, **48–49** (1991) 253.
(k) W. Spaleck, M. Antberg, V. Dolle, R. Klein, J. Rohrmann and A. Winter, *New J. Chem.*, **14** (1990) 499.
- (a) S. Miya, T. Mise and H. Yamasaki in K. Tominaga, K. Soga (eds.) *Catalytic Olefin Polymerization* Elsevier, Amsterdam, 1990, p. 531.
- (a) E.B. Coughlin and J.E. Bercaw, *J. Am. Chem. Soc.*, **114** (1992) 7606–7607.
(b) R.E. Marsh, W.P. Schaefer, E.B. Coughlin and J.E. Bercaw, *Acta Crystallogr., Sect. C*, **48** (1992) 1773–1776.
- W.A. Herrmann, M.J.A. Morawietz and Priermeier, *Angew. Chem., Int. Edn. Engl.*, **33** (1994) 1946.
- (a) R.L. Haltermann and T.M. Ramsey, *Organometallics*, **12** (1993) 2879.
(b) W.W. Ellis, T.K. Hollis, W. Odenkirk, J. Whelan, R. Ostrander, A.L. Rheingold and B. Bosnich, *Organometallics* **12** (1993) 4291.
(c) M.E. Huttenloch, J. Diebold, U. Rief, H.H. Brintzinger, A.M. Gilbert and T.J. Katz, *Organometallics*, **11** (1992) 3600.
- (a) M.J. Burk, S.L. Colletto and R.L. Haltermann, *Organometallics* **10** (1991) 2998.

- (b) Z. Chen and R.L. Haltermann, *J. Am. Chem. Soc.*, **114** (1992) 2276.
- (c) T.K. Hollis, A.L. Rheingold, N.P. Robinson, J. Whelan and B. Bosnich, *Organometallics*, **11** (1992) 2812.
- (d) A.L. Rheingold, N.P. Robinson, J. Whelan and B. Bosnich, *Organometallics*, **11** (1992) 1869.
- (e) J.A. Bandy, M.L.H. Green, I.M. Gardiner and K.J. Prout, *J. Chem. Soc., Dalton Trans.*, (1991) 2207.
- [9] W. Mengele, J. Diebold, C. Troll, W. Röhl, H.H. Brintzinger, *Organometallics* **12** (1993) 1931.
- [10] R.B. Grossman, J.-C. Tsai, W.M. Davis, A. Gutiérrez and S.L. Buchwald, *Organometallics*, **13** (1994) 3892.
- [11] *rac*-BpZrCl₂ was first prepared using an analogous procedure at the Polymers Group, Exxon Chemical Company, Baytown, TX; see T. Burkhart, private communication, 1994.
- [12] G.M. Diamond, S. Rodewald and R.F. Jordan, *Organometallics*, in press.
- [13] T.A. Herzog, M.B. Abrams and J.E. Bercaw, unpublished results, 1995.
- [14] L.E. Manzer, J. Deaton, P. Sharp and R.R. Schrock, *Inorg. Synth.*, **21** (1982) 135.
- [15] A.C. Larson, *Acta Crystallogr.* **23** (1967) 644.
- [16] D.J. Duchamp, The CRYM crystallographic computing system, *American Crystallographic Association Meet. Bozeman, MT, 1964*, American Crystallographic Society, New York, 1964, Paper B14, 29–30.
- [17] C.K. Johnson, ORTEP II, *Rep. ORNL-5138*, 1976 (Oak Ridge National Laboratory, Oak Ridge, TN).
- [18] (a) D.T. Cromer, *International Tables for X-ray Crystallography*, Vol. IV, Kynoch, Birmingham 1974, pp. 149–151.
(b) D.T. Cromer and J.T. Waber, *International Tables for X-ray Crystallography*, Vol. IV, Kynoch, Birmingham, 1974, pp. 99–101.